DEVELOPMENT OF AIRFOIL SECTIONS FOR THE SWEPT-BACK TAILLESS SAILPLANE SB 13

Presented at the XIX. OSTIV Congress, Rieti, Italy (1985)
by Clemens Schürmeyer, Akademische Fliegergruppe Braunschweig, Germany
and Karl-Heinz Horstmann, DFVLR, Braunschweig, Germany

Summary

For the tailless swept wing sailplane SB 13 special airfoil properties are required. For these requirements several airfoils have been designed and analyzed by a subsonic potential flow boundary layer interaction method.
Additionally some stability calculations of the laminar boundary layer have been done.
The airfoils have been tested in free-flight conditions in the flying testbed on the sailplane "JANUS" of the DFVLR in Braunschweig. The results of the theoretical calculations, of the free-flight measurements and the comparison of both are shown.
In comparison with other airfoils, the airfoils for the tailless sailplane SB 13 have the same lift and drag characteristics. There is no special disadvantage of this special pitching-moment-free airfoil sections.

Introduction

Tailless planes, sometimes also called "FLYING WINGS", have always been a challenge in airplane design. They probably offer a great potential in performance compared with conventional designs because of less surface area and less weight. But tailless sailplanes never showed the success one might expect in contrast to the conventional planes, which have achieved a very high technological level during the last 20 years, mainly due to composite materials and improved aerodynamics. The main designers of tailless sailplanes up to 1960 were A. LIPPISCH, the HORTEN BROTHERS and CHARLES FAUVEL. Since that time the development has stopped.
With conventional sailplanes further improvements can be expected only by small detail modifications or expensive projects like variable wing geometry. For this reason an unconventional design concept like the tailless wing was launched by "Akademische Fliegergruppe Braunschweig" in 1983. This project for the 15 meter standard class called SB 13 shows calculated performance improvements up to 10% compared to existing conventional sailplanes.
Additionally to the control- and stability functions the induced drag is reduced by using the vertical tail as winglets.
To reach the desired high performance it is necessary to design low pitching moment airfoils with the same low drag as conventional laminar flow airfoils. This seems to be possible because airfoil sections with longer laminar flow boundary layer on the lower surface show lower pitching moments.

Symbols

c	airfoil section chord
c_d	drag coefficient
c_l	local lift coefficient
c_L	total lift coefficient
c_p	pressure coefficient
N	logarithm of the amplification factor
Re	Reynolds number
α	Angle of attack
η_E	(elevator) flap angle
ϕ	leading edge sweep angle

Airfoil requirements

The catalog for the requirements is based on the design study made by POTTHOFF (1). Figure 1 shows a 3-side view. The wing is fitted with winglets. In regard

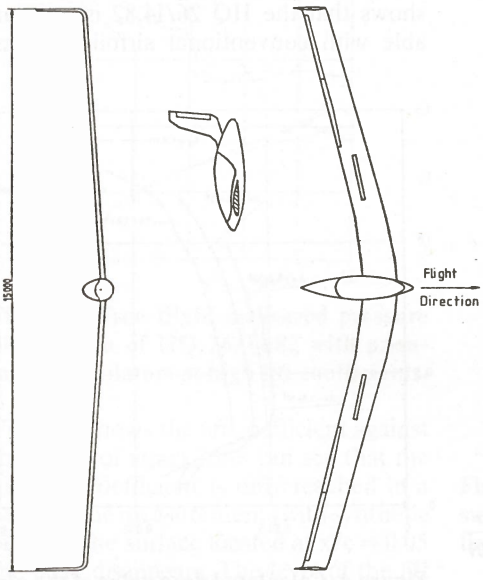

Figure 1. 3-side view of the tailless sailplane project SB 13.

to good control and stability characteristics the wing has a sweep angle of 15.6 degrees. Near the root the sweep is reduced in order to improve the pilots view and to reduce the flutter problem. Elevator and aileron are integrated in the two flaps at the outer part of the wing. Hence, two different airfoil sections are required for the SB 13, a fixed one for the inner wing and a flaped one for the outer wing. The lift distribution of the SB 13 planform is shown in Fig. 2 for total lift coefficients of $c_L = 0.3/1.2$ at high and low speed respectivly.

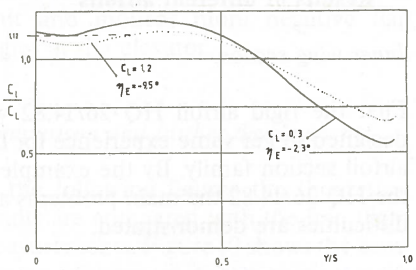

Figure 2. Calculated lift distribution of the SB 13 wing planform (1).

For the inner wing the local lift coefficient is nearly 10% higher than the total lift coefficient. At a wingloading of 270 N/m^2 and a main speed range from 70 km/h to 160 km/h the lift coefficient at the limits of the laminar drag bucket are $c_l = 0.3/1.3$ for the inner airfoil section.
The greatest problem of the outer part is the elevator flap because it has to work in the opposite way of a camber flap to reach the moment balance. So a high lift coefficient is necessary at negative flap angles and a low lift coefficient at flap angles of nearly zero. Hence, a large laminar drag bucket is required from $c_l = 0.2$ to $c_l = 1.4$ based on a flap angle of zero.
The main requirement for the airfoils is the low pitching moment. It is possible to compensate the pitching moment of the airfoil by twisting the wing. But there is a limit of $/c_m/ \leqq 0.01 - 0.02$ for the pitching moment based on the 1/4 chord should the induced drag not rise by the influenced of the twist angle.
For a good airfoil the following general requirements should be fulfilled:

- good stall characteristics →
  at the maximum lift coefficient the value of c_l should not decrease rapidly over a certain range of angle of attack
- the influence of bugs and rain shouldn't change the following values rapidly:
  - maximum lift coefficient →
    otherwise the stall speed increases and it becomes more difficult to

circle in thermals because the radius is too large. Also the landing speed will be higher.
- pitching moment →
  if the pitching moment increases larger negative flap angles are required to reach the moment balance. So it can be possible that the limit, where the flaps do not work is passed over.
- Drag coefficient →
  the drag of laminar flow airfoils normally increases, when the transition occurs more and more upstream influenced by bugs or rain. But there should not be additional drag from turbulent separation influenced by the transition located near the leading edge.

Results of different airfoils

Inner wing section

First the rigid airfoil HQ 26/14.82 was designed to get some experience for this airfoil section family. By the example of the HQ 26/14.82 the main problems and difficulties are demonstrated.

Theoretical calculation

The airfoils are analyzed by a subsonic potential flow boundary layer interaction method, which is based on the work of EPPLER/SOMERS (2) and an extension by the DFVLR in Braunschweig (3,4).
Figure 3 shows the theoretical pressure distribution of the HQ 26/14.82 airfoil.

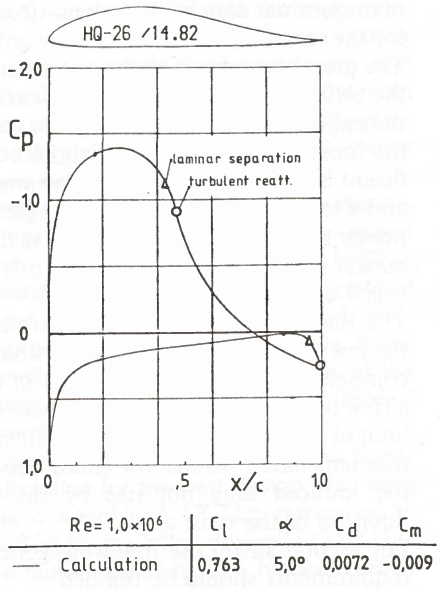

Figure 3. Theoretical pressure distribution of the airfoil HQ 26/14.82.

The conspicuous difference between this pressure distribution and one of a conventional laminar flow airfoil is the negative lift at the aft 20%. This is necessary to get the low pitching moment. The minimum pressure is at 30% on the upper surface followed by a very short destabilizing region. The theoretical results show a small laminar separation bubble. If this bubble induces additional drag, there is the opportunity to destroy the bubble with pneumatic turbulators. The pressure gradient of the last 50% is calculated in a way that the shape factor is just underneath the value of turbulent separation. This leads to concave pressure distribution which allows the highest pressure rise without turbulent separation, as described by STRATFORD (13).
On the lower surface a long laminar boundary layer flow is useful, first to compensate the higher friction drag of the upper surface and second to get a low pitching moment.
Up to 90% of chord there is a negative pressure gradient and consequently laminar flow. The pressure rise starts without any destabilizing region. Hence, there must occur a laminar separation. There at 90% chord on the lower side it is necessary to have turbulators to prevent the additional drag of the laminar separation bubble.
The pressure gradient of the last 10% of the chord is low and does not cause any turbulent separation if the transition, influenced by bugs or else, occurs at the leading edge!
The calculated value of the pitching moment is not very reliable, because the method can not calculate the influence of bubbles on the pressure distribution and because, as in all methods, the value of the trailing edge pressure is incorrect. The calculated value $c_m = -0.009$ is inside of the limit of the SB 13.
The results of the calculated polar at Reynolds numbers 1.0 to 2.5 × 10^6, Fig. 4, shows that the HQ 26/14.82 is comparable with conventional airfoil sections.

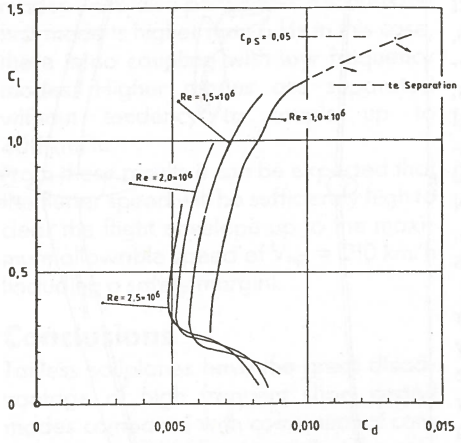

Figure 4. Calculated drag polar of the airfoil HQ 26/14.82.

The minimum drag at Re = 2.5 × 10^6 is $c_d \leqq 0.005$. The broken line in the higher region of the polar indicates turbulent separation on the rear part of the upper surface. According to experience the maximum lift coefficient will be reached, if the calculated turbulent separation is indicated at a pressure coefficient of $c_p = 0.05$. Hence the curve has to be corrected to higher drag and lower lift coefficients. The range of the laminar drag bucket from $c_l = 0.3$ up to $c_l = 1.35$ seems to be achieved. To simulate the influence of bugs or rain some calculations are made with transition at 7% on both surfaces. No turbulent separation is indicated at intermediate and low lift coefficients but the value of the drag coefficient is doubled.
At all calculations considered so far only the laminar turbulent transition induced by the Tollmien-Schlichting instability was taken into account. For unswept wings the Tollmien-Schlichting instability is the only mode leading to transition. With swept wings transition additionally can be caused by crossflow. Figure 9 shows crossflow stability calculations on the HQ 26/14.82 upper surface at different leading edge sweep angles. The so called N-factor is the logarithm of the amplification factor of the disturbances. Comparisons of calculations and measurements show that at the value of N ≅ 10 the transition is caused by crossflow. The figure shows clearly that at a sweep angle of 16° there is no danger of crossflow induced transition. Crossflow transition can be expected at sweep angle of more than 40 degrees.
All the calculated results shows a positive view of this airfoil section.

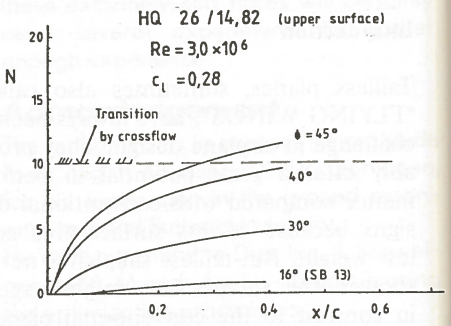

Figure 9. Crossflow stability calculation on the HQ 26/14.82 upper surface at different leading edge sweep angle ϕ.

Free flight-measurements

The measurements at Reynolds numbers from 1.0 up to 2.0 × 10^6 have been made in free-flight condition in the flying testbed on the sailplane "JANUS" of the DFVLR Braunschweig. The chord of the modell is 650, the span is 2000 mm so that the geometry aspect ratio is = 3.1. Additionally both sides of the modell are fitted with endplates.
For some tests pneumatic turbulators are used. In order to prevent laminar separation bubbles, the air jets should operate in the vicinity of the separation line as shown in references (5) and (6). The jets of air are produced by small tubes with an internal diameter of 0.6 (mm) which are spaced in spanwise direction with intervals of 1.6 - 3.2% of the wing chord.

The air for the jets is supplied by an internal duct with total pressure which if necessary can be reduced by suitable devices, thereby reducing the volume of air emerging from the jet orifices. Pneumatic turbulators offer the further advantage that they are still active in the region behind the laminar separation (9).
Measured pressure distributions are shown in figure 5. The continous line shows the result with clean surface, the broken one with turbulators. On both surfaces laminar separation bubbles are indicated. On the lower surface without turbulators there is a characteristic pressure increase in front of the laminar separation and a pressure flattering behind as described in (7). The characteristic steep pressure rise at the rear part of the bubble is missed because the flow is separated up to the trailing edge. The laminar separation bubble on the upper surface seems not to be destroyed by the turbulators. The turbulator position seems to be to far behind the laminar separation line.

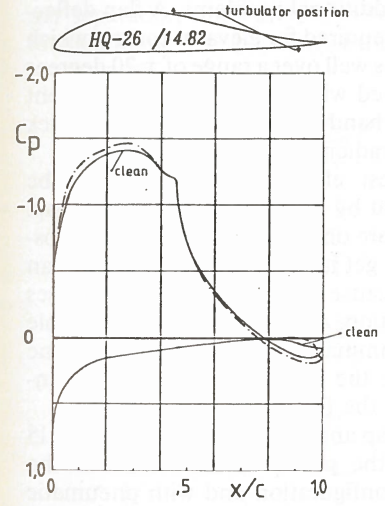

Re = 1,0×10⁶	c_l	α	c_d	c_m
clean surface	0,804	4,7°	0,0081	-0,025
with turbulat.	0,816	5,2°	0,0076	-0,012

Figure 5. Free-flight measured pressure distribution of the airfoil HQ 26/14.82 with and without pneumatic turbulators.

The influence of the turbulators on the drag is given in Figure 6. For the Reynolds number of 1.0×10^6 the drag is considerably reduced by the turbulators, located at x/c = 0.895 on the lower surface. The drag reduction decreases with increasing lift coefficient. A remarkable drag reduction due to the turbulators on the upper surface at x/c = 0.44 can be seen at intermediate lift coefficients.
If the lift coefficient increases the difference in drag will disappear, as a result of destabilization of the flow in front of the separation by a leading edge pressure peak. If transition occurs upstream of the turbulator position and hence the turbulators disturb the turbulent boundary layer, it is remarkable that pneumatic turbulators do not cause any additional drag.

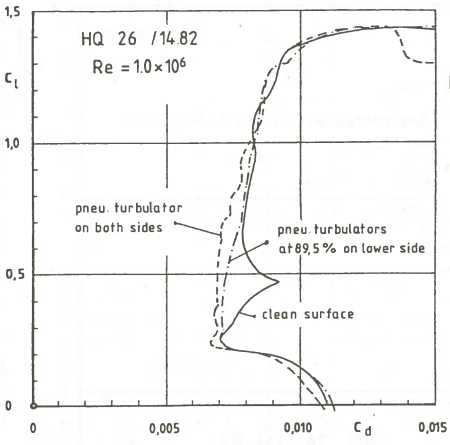

Figure 6. Results of free-flight measurements on HQ 26/14.82 with and without pneumatic turbulators.

The lower limit of the laminar drag bucket correspond to the requirements. The upper limit is higher than expected. Up to the lift coefficient of $c_l = 1.4$ there is no turbulent separation indicated in the measured pressure distribution of the upper surface. But when the angle increases the separation suddenly moves upstream to 40–50% of chord on the upper side (Fig. 7). One reason for this effect is the concave shape with the so called STRATFORD-pressure distribution as described above.

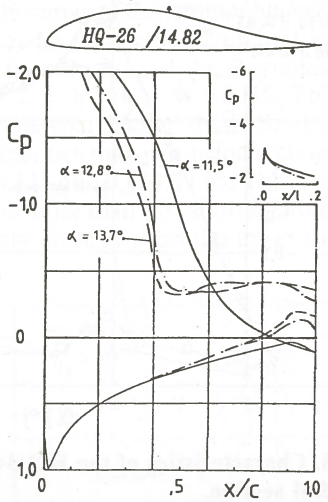

Figure 7. Free-flight measured pressure distribution of HQ 26/14.82 with pneumatic turbulators at high lift coefficients.

Figure 8 shows the lift coefficient against the angle of attack, one can see that the high lift coefficient is only reached in a peak. In the measurements with synthetic bugs on the surface located at x/c = 0.05 the peak disappears. The level of the lift coefficient at high angles of attack is equal to the measurements without synthetic bugs.
The pitching moment at zero lift coefficient is $c_m = -0.01$. This is below the limit of $|c_m| \leqq 0.02$. The gradient of pitching moment against angle of attack shows the center of pressure at $x/c \cong 0.26$. With synthetic bugs the pitching moment behaviour is nearly the same, but the absolute

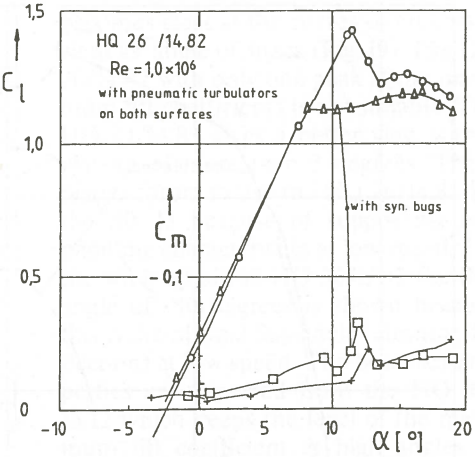

Figure 8. Characteristics of the HQ 26/14.82 airfoil section.

values are higher. This is at the required limit and induces more negative flap angles at the elevator.

Comparison and further development

In the following figures the theoretical results are compared with the free flight measurements. Figure 10 shows the comparison of pressure distributions at a lift coefficient at $c_l = 0.77$. The measurement has been done with pneumatic turbulators on both surfaces. A remarkable difference can be seen at the aft 10%. The calculated trailing edge pressure is higher than the measured one. This is a well-known mistake of all potential flow boundary layer interaction methods.

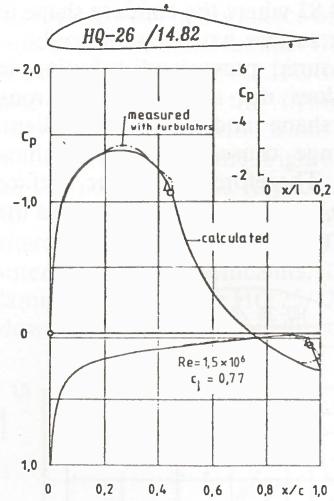

Figure 10. Comparison between measured and calculated pressure distribution of HQ 26/14.82.

The comparison of both polars shows a good agreement up to the lift coefficient of $c_l = 1.1$ (Fig. 11). At higher lift coefficients the calculated drag is normally lower than the measured one. But in this case it is contrary. This could be a result of the pressure drag. At the rear 15% of the upper surface of the airfoil HQ 26/14.82 is nearly parallel to incident flow so that the pressure has no component in the direc-

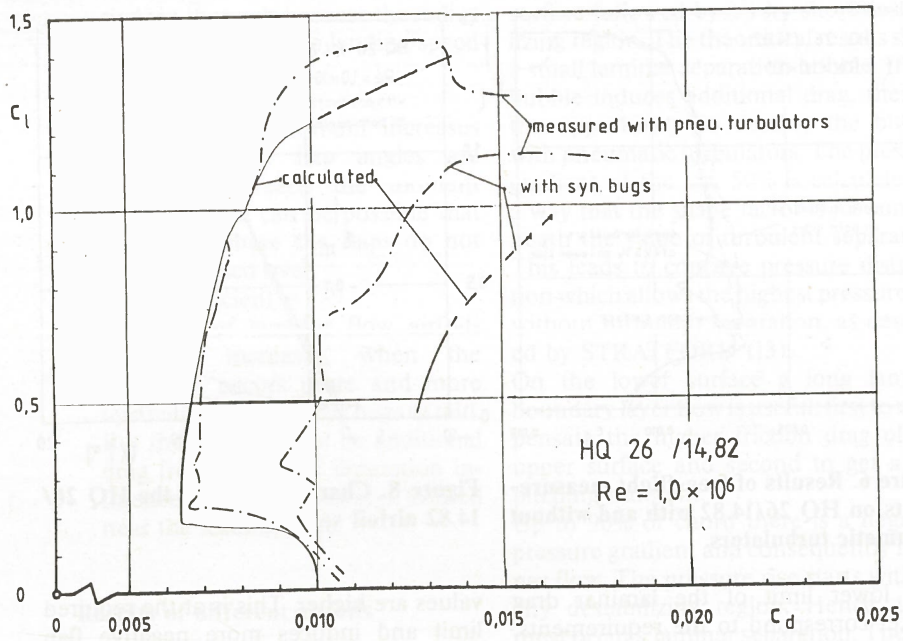

Figure 11. Comparison between measured and calculated drag polar of HQ 26/14.82 at Re = 1.0 × 10^6 with and without bugs.

tion of drag. The calculated pressure drag is a function of the displacement thickness.

With the exception of high lift coefficients there is a good correlation between calculation and measurement. The indicated turbulent separation must not be one with dead flow. It could also be a sign of larger change in the displacement thickness development.

The result of the HQ 26/14.82 indicates that it is possible to design further airfoils for the requirements of the SB 13. A further development of this airfoil is the HQ 34/14.83 where the concave shape of the upper surface has been reduced.

The measured pressure distribution in Fig. 12 does not show such a strong concave shape and pressure gradient. This change causes a higher pitching moment. Therefore the lower surface must also be changed to compensate the pitching moment.

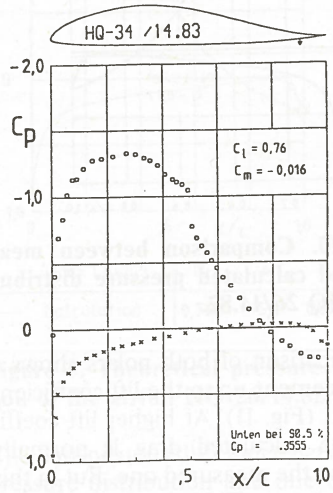

Figure 12. Free-flight measured pressure distribution of HQ 34/14.83 at Re = 1.0 × 10^6 with pneumatic turbulators located at 90% on the lower surface.

In Figure 13 it can be seen that this modification was correct. There is not only one peak at the maximum lift coefficient, it is a plateau over more than 3 degrees before the lift coefficient decreases. The turbulent separation does not move upstream as fast as the HQ 26/14.82.

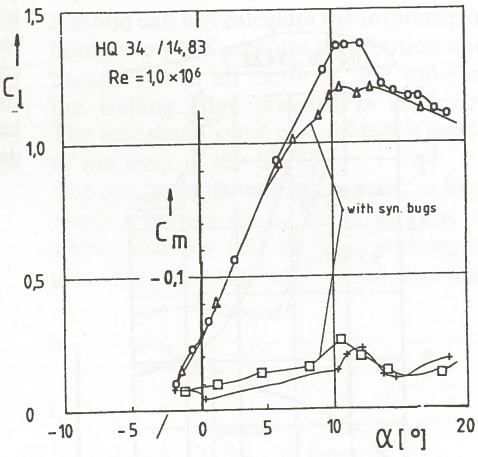

Figure 13. Characteristics of the HQ 34/14.83 airfoil section.

At a lift coefficient of zero and without bugs the pitching moment is $c_m = -0.01$ and with them it grows to $c_m = -0.02$. In both cases the pitching moment is inside the limit. The change of the pitching moment by bugs is lower than measured at the HQ 26/14.82.

The polar with pneumatic turbulators at x/c = 90% (Fig. 14) shows a laminar bucket from $c_l = 0.3$ up to $c_l = 1.35$. The minimum drag at a Reynolds number of 2 × 10^6 is nearly $c_d \cong 0.005$. The unsteadiness of the polars at lower Reynolds numbers is a result of a small laminar bubble on the upper surface. Further small drag reduction will be possible by using turbulators located at 40% chord on the upper side. This option was not measured.

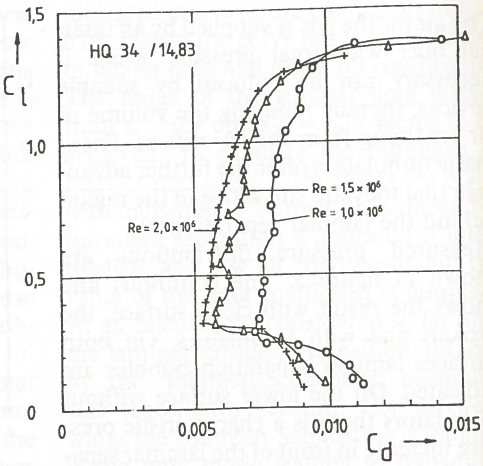

Figure 14. Results of free-flight measurements on the HQ 34/14.83 with pneumatic turbulators located at 90% on the lower surface.

Results of the outer wing section (with flap)

For the wing tip airfoil section there are some additional problems. A flap deflection is required for elevator control which operates well over a range of ± 20 degrees combined with the correct flap moment for the hand force, to get a positive stick force gradient against the speed.

The best efficiency of a flap can be achieved by means of a 20% chord flap. Therefore on the lower side it is not possible to get laminar flow over more than 80% because the flap slot normally causes a transition. Additionally it is not possible to get laminar flow on the flap every time because the pressure gradient is dependent of the flap deflection.

For a flap angle of zero degrees Figure 15 shows the pressure distribution in the clean configuration and with pneumatic turbulator at 82% on the lower side. The upper side looks similar to the HQ 26/14.82 and HQ 34/14.83 with a laminar

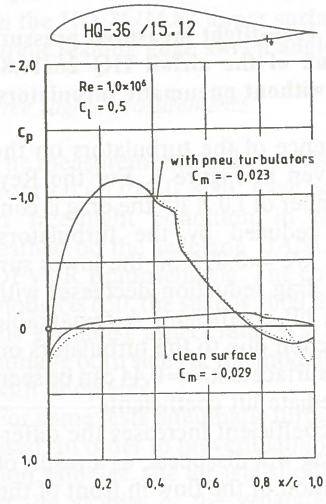

Figure 15. Measured pressure distribution of the airfoil HQ 36/15.12 at a flap deflection of zero with and without pneumatic turbulators located at 82.5% on the lower surface.

separation between 42% and 48%. On the lower surface the pressure rise begins at 80%. The clean configuration presents a laminar separation beginning at 82% without any reattachment. With pneumatic turbulators the bubble disappears. For low pitching moment negative lift is needed over the whole flap, but the desirable hand force gradient does not allow the corresponding positive flap moment. Therefore at the aft 50% of the flap positive lift is indispensable. This is a compromise between flap moment and pitching moment. The pitching moment of $c_m = -0.023$ is a little bit outside of the preset range.

For positive flaps angles down to -10 degrees the pneumatic turbulators work well. At lower flap angles there is a laminar separation on the lower surface in spite of pneumatic turbulators. At a flap deflection of $\eta_E = -15$ degrees the turbulators effect transition down to an angle of attack of 7 degrees (Fig. 16). But at lower angles of attack the pneumatic turbulators are ineffective. In this case the laminar separation starts at 75% without any reattachment. The position of the turbulators is far downstream from the point of separation and the direction of the jets is backward. Apparently the energy of the air jets is not sufficient in this case. The change in the pressure distribution is remarkably heavy. This effect can be seen in Figure 17. At a flap angle of $\eta_E = -20$ degrees there is a laminar separation on the lower surface over the whole measured range. To prevent the laminar separation and to reach flap efficiency at negative flap angles turbulators in a more upstream position are required.

In this forward turbulator positon at x/c = 0.72 Zick-Zack-Tape is used. Without a bubble the curve moves to lower lift coefficients for a flap angle of -20 degrees and the peak disappears at high lift coefficients. The flap efficiency is now linear over the flap range of ± 20 degrees.

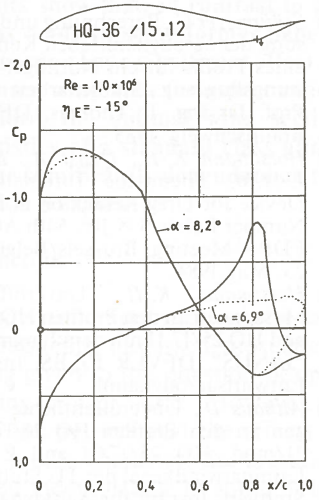

Figure 16. Measured pressure distribution of the airfoil HQ 36/15.12 at a flap deflection of -15 degrees with pneumatic turbulators located at 82.5% on the lower surface.

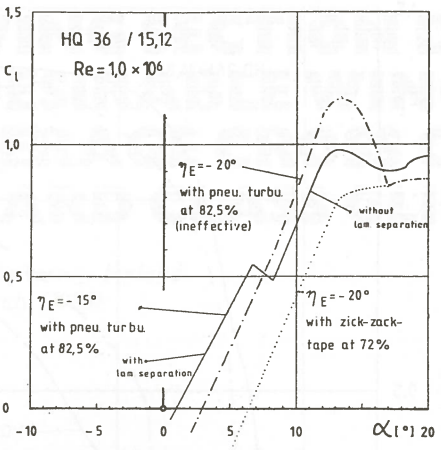

Figure 17. Characteristics of the HQ 36/15.12 airfoil section.

It is also possible to use pneumatic turbulators, but in the model there was no provision for air jets in this position.

The Zick-Zack-Tape influences the laminar boundary layer flow in a way, that transition occurs ≅ 4% chord later. Inside the laminar boundary layer probably Tollmien-Schlichting waves are excited also the in spanwise direction causing transition after some wave lengths (4% chord). The polar of HQ 36/15.12 is given in figure 18 for a flap angle of zero degrees. The range of the laminar bucket probably reaches from $c_l = 0.2$ up to $c_l = 1.4$. The minimum drag at the Reynolds number of 2×10^6 is $c_d \cong 0.0055$. This drag is somewhat higher than the drag of the other two midspan airfoil sections HQ 26/14.82 and HQ 34/14.83. This is a result of the more than 10% shorter laminar boundary layer flow on the lower surface.

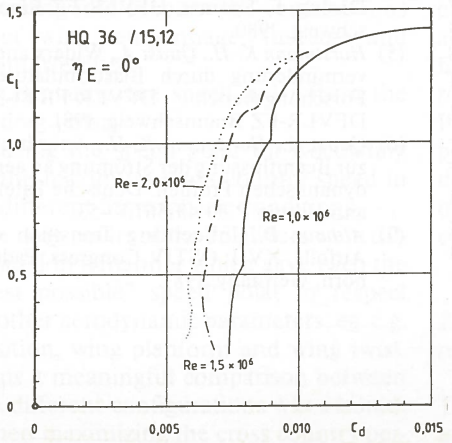

Figure 18. Drag polar of the HQ 36/15.12 at a flap deflection of zero with pneumatic turbulators at 82.5%.

Application of these airfoils for the SB 13

The main reason to design a second rigid airfoil were the bad properties of the HQ 26/14.82 at high lift coefficients. This difference in properties at low speed becomes clear at the curves of lift coefficient vs. angle of attack (Fig. 19). The HQ 26/14.82 with only one peak at the maximum lift coefficients is not suitable. The HQ 34/14.83 gives a better view with a plateau of more than 3 degrees. These results forbid to use the HQ 26/14.82 for the SB 13 because of supposedly bad handling characteristics at low speed. For the wing tip airfoil HQ 36/15.12 the flap angle of -10 degrees is shown because this is the normal flap angle (elevator deflection) at low speed. The best stall properties are expected from the HQ 36/15.12 which keeps the level of the maximum lift coefficient at high angles of attack. In the case of tailles sailplane there is no demand for very high lift coefficient at wingtip.

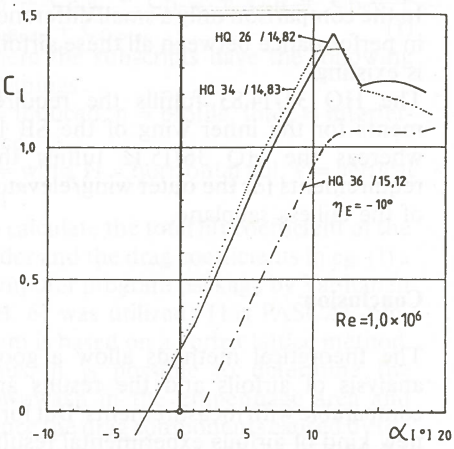

Figure 19. Characteristics of different airfoils for the SB 13 projet.

To compare the performance of these airfoils to conventional laminar flow airfoils the rigid airfoil HQ 25/17.11 is used. It was also measured on the flying testbed "JANUS" but the airfoil is not used in a standard class sailplane. Figure 20 shows all the polars for one Reynolds number $Re = 1.5 \times 10^6$. Between the rigid airfoils there is not any remarkable difference at intermediate lift coefficients. The whole laminar bucket of the HQ 25/17.11 is shift down by $\Delta c_l = 0.1$. At high lift coefficients

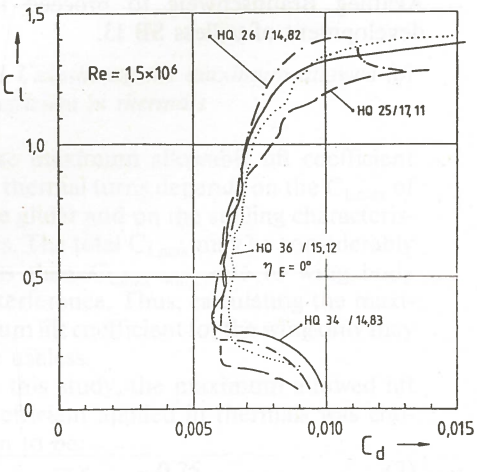

Figure 20. Free-flight measured drag polars of different airfoils.

the HQ 34/14.83 has a little more drag than the HQ 26/14.82 but this difference is neglectable because of the high induced drag at low speed. Over the whole polar the drag of the HQ 36/15.12 is higher than the other airfoils! The higher drag of $\Delta c_d = 0.00005$ is a result of larger laminar bucket and the 20% flap.

To compare an airfoil used in a standard class sailplane the polar of the HQ 26/14.82 and HQ 21/17.15, both measured in the laminar windtunnel in Stuttgart is presented in figure 21. The HQ 21/17.15 is used in the Falcon, a prototype built by H. STREIFENEDER. The modified airfoil HQ 21/mod is used in the DG 300. The clean configuration of the HQ 26/14.82 is in all parts a little bit better than the HQ 21/mod. With synthetic bugs it is contrary.

In the comparison only a small difference in performance between all these airfoils is existing.

The HQ 34/14.83 fulfills the requirements for the inner wing of the SB 13 whereas the HQ 36/15.12 fulfills the requirements for the outer wing/elevator of the tailless sailplane.

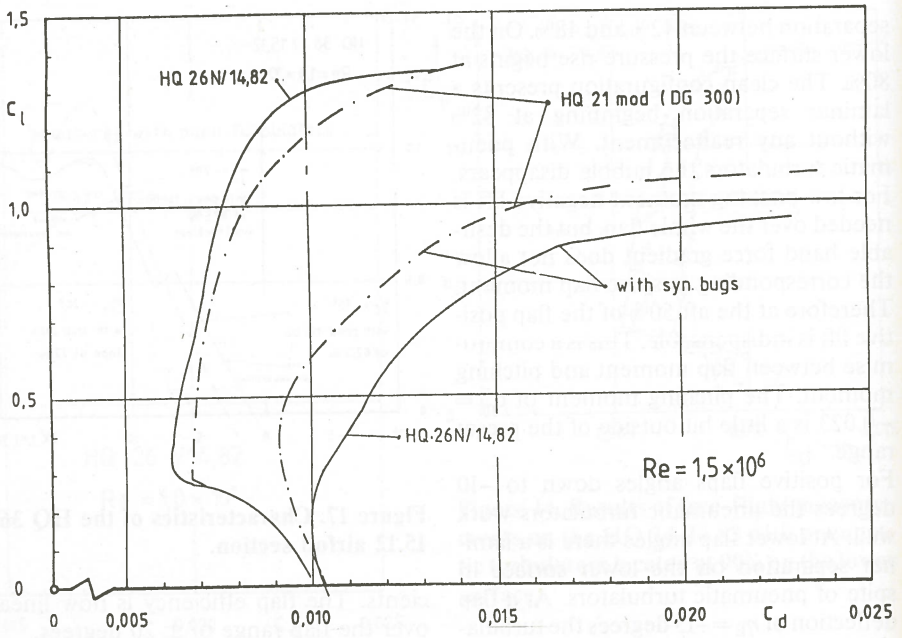

Figure 21. Results of windtunnel measurements of different airfoils at Re = 1.0 × 10^6 with and without bugs.

Conclusion

The theoretical methods allow a good analysis of airfoils and the results are comparable with measurements. But for a new kind of airfoils experimental results are necessary to check the theoretical methods. In this case it was the concave pressure distribution where the theoretical results were intepreted wrong until the first measurements were made.

For the tailless sailplane SB 13 of Akaflieg Braunschweig three airfoil sections were designed and measured in free flight. The low-pitching moment condition does not affect the drag. In comparison with conventional airfoils section the drag is even somewhere lower, the extension of low drag bucket (laminar bucket) being the same. To achieve the low drag turbulators must be used on upper and lower surface of the airfoils. Results of calculation and free flight measurements encourage Akaflieg Braunschweig to proceed in development of tailless SB 13.

References

(1) *Potthoff U.*, Berechnung zum Problem des Nurflügel-Segelflugzeuges. Studienarbeit Nr. 83/1 Prof. Dr.-Ing. F. Thomas, DFVLR-FZ Braunschweig, 1983.

(2) *Eppler R., Somers R.M.*, A Computer Program for the Design and Analysis of Low-Speed Airfoils. NASA TM 80210, 1980.

(3) *Radespiel R.*, Erweiterung eines Profilberechnungsverfahrens in Hinblick auf Entwurfs- und Nachrechnungen von Laminarprofilen für Verkehrsflugzeuge. Diplomarbeit Nr. 81/3 Prof. Dr.-Ing. F. Thomas, DFVLR-FZ Braunschweig, 1981.

(4) *Kohlmeier H.H.*, Berücksichtigung der Verdrängungswirkung der Grenzschicht bei Berechnung der Druckverteilung von Profilen. Studienarbeit Nr. 80/2 Prof. Dr.-Ing. F. Thomas, DFVLR-FZ Braunschweig, 1980.

(5) *Horstmann K.-H., Quast A.*, Widerstandsverminderung durch Blasturbulatoren. Forschungsbericht DFVLR-FB-81-33, DFVLR-FZ Braunschweig, 1981.

(6) *Quast A., Horstmann K.-H.*, Anordnung zur Beeinflussung der Strömung an aerodynamischen Profilen. Deutsche Patentanmeldung P 30 43 567.7.-53.

(7) *Althaus D.*, Influencing Transition on Airfoils. XVII. OSTIV Congress, Paderborn, Germany, 1981.

(8) *Schürmeyer C.*, Berechnung und Vermessung der aerodynamischen Kenngrößen eines Profils für ein Nurflügel-Hochleistungsflugzeug. Studienarbeit Nr. 84/1 Prof. Dr.-Ing. F. Thomas, DFVLR-FZ Braunschweig, 1985.

(9) *Horstmann K.-H., Quast A., Boermans L.M.M.*, Pneumatic Turbulators - A Device for Drag Reduction at Reynolds Number Below 5 × 10^6. 54th AGARD - FDP - Meeting, Brussels/Belgium, 21 - 23. May 1984.

(10) *Horstmann K.-H.*, Unveröffentlichte Messungen an den Profilen HQ 36/15.12 and HQ 25/17.11 mit dem Flugmeßträger "JANUS". DFVLR FZ-BS, Institut für Entwurfsaerodynamik.

(11) *Althaus D.*, Unveröffentlichte Messungen an den Profilen HQ 21/17.15, HQ 21/mod, HQ 25/17/11 and E 580 im Laminarwindkanal der TU Stuttgart. TU Stuttgart, Institut für Aerodynamik und Gasdynamik.

(12) *Althaus D.*, Polarenmessungen am Profil HQ 26/14.82. Institutsbericht Juli 84, Institut für Aerodynamik und Gasdynamik, TU Stuttgart.

(13) *Stratford B.S.*, An experimentel Flow with Zero Skin Friction throughout it's Region of Pressure Rise. F.F.M. Volume 5, 1959.